

Short communication

A novel electrochemical process to prepare a high-porosity manganese oxide electrode with promising pseudocapacitive performance

Jeng-Kuei Chang^{a,*}, Shih-Hsun Hsu^b, Wen-Ta Tsai^a, I-Wen Sun^b

^a Department of Materials Science and Engineering, Frontier Material and Micro/Nano Science and Technology Center, National Cheng Kung University, 1Ta-Hsueh Road, Tainan 701, Taiwan

^b Department of Chemistry, National Cheng Kung University, Tainan, Taiwan

Received 15 August 2007; received in revised form 9 November 2007; accepted 12 November 2007

Available online 21 November 2007

Abstract

A nanoporous nickel (Ni) substrate was successfully prepared by selective dissolution of copper (Cu) from a Ni–Cu alloy layer. It was noted that both the Cu etching and the Ni/Cu codeposition processes could be performed in the same solution. Afterwards, anodic deposition was carried out to disperse fibrous manganese (Mn) oxide onto the nanoporous Ni substrate. As a result, a novel oxide electrode with a high-porosity structure was fabricated by the totally electrochemical procedure, which is very simple and efficient. Pseudocapacitive performance of this oxide electrode was evaluated by cyclic voltammetry in 0.1 M Na₂SO₄ solution. The data indicated that specific capacitance of the Mn oxide was as high as 502 F g⁻¹, which was 85% higher than that deposited on a flat electrode. Capacitance retained ratio after 500 charge–discharge cycles of the Mn oxide was also significantly improved from 75 to 93% due to the use of the nanoporous substrate.

© 2007 Elsevier B.V. All rights reserved.

Keywords: Supercapacitor; Mn oxide; Porous material; Selective dissolution

1. Introduction

Electrochemical supercapacitors are the charge-storage devices that have a greater power density and longer cycle life than batteries, and they possess a higher energy density as compared with conventional capacitors [1]. The natural abundance and low cost of Mn oxide, accompanied by its satisfactory electrochemical performance in mild electrolytes and environmental compatibility, have made it one of the most promising electrode materials for supercapacitors. Owing to the fast, continuous, and reversible redox reaction of Mn oxide, pseudocapacitive behavior of the electrode can be recognized [2–4]. Since the capacitance of Mn oxide is associated with the reversible faradaic reaction between its trivalent and tetravalent states [3–5], the theoretic specific capacitance should be above 1100 F g⁻¹. However, both the poor electronic and ionic conductivity of Mn oxide have kept itself from approaching the ideal electrochemical performance [6,7]. The typical spe-

cific capacitances of Mn oxides reported in the literature are in the range of 100–250 F g⁻¹ [2,6–12] except those extremely thin oxide films [3,4]. In order to promote the utilization and reactivity of Mn oxide, and hence further improve its pseudocapacitive performance, two kinds of nanotechnologies have been adopted. (i) Using anodic aluminum oxide (AAO) templates to prepare Mn oxide nanowire arrays [13–15]. The ordered Mn oxide with high aspect ratio and high surface area was found to have a specific capacitance of 254 F g⁻¹, as reported by Xu et al. [15]. (ii) Using carbon nanotubes (CNTs) to fabricate the Mn oxide/CNTs composite electrodes [16–19]. The Mn oxide was highly dispersed onto the CNTs, which could provide electronic conductive paths and form a network of open mesopores as well. According to the data reported by Lee et al. [19], the oxide specific capacitance was as high as 415 F g⁻¹. However, both the processes related to AAO and CNTs are too complicated and expensive to be used in practical applications. On the other hand, a nanoporous Ni electrode prepared by a simple dealloying process was demonstrated by Sun et al. [20]. This paper would like to further propose a novel and totally electrochemical procedure to construct a high-porosity (and hence high surface area) Mn oxide electrode with a nanoporous Ni substrate. The

* Corresponding author. Tel.: +886 6 2757575x62942; fax: +886 6 2754395.
E-mail address: catalyst@mail.mse.ncku.edu.tw (J.-K. Chang).

promising pseudocapacitive performance of this electrode will be demonstrated.

2. Experimental

The Ni–Cu alloy films were electrodeposited from a plating solution containing 1 M NiSO₄, 0.01 M CuSO₄ and 0.5 M H₃BO₃ (pH 4). The deposition process was performed at 25 °C in a three-electrode cell with a platinum counter electrode and a saturated calomel reference electrode (SCE, +0.241 V versus SHE). The indium-doped tin oxide (ITO) coated glass with exposed area of 1.4 cm² was assembled as the working electrode. The alloy films were deposited under a constant potential condition, and the total cathodic passed charge was controlled to be 1 C. Selective dissolution of Cu from the alloy was then conducted in the same solution by applying an anodic potential of 0.5 V till a cutoff current density of 10 μA cm⁻². Consequently, a porous Ni electrode was obtained. The morphologies and chemical compositions of the samples were examined with a scanning electron microscope (SEM, Philip XL-40 FEG) and its auxiliary X-ray energy dispersive spectroscopy (EDS).

Mn oxide was anodically deposited onto the prepared porous Ni substrate in 0.5 M Mn(CH₃COO)₂ aqueous solution. An anodic potential of 0.5 V (versus SCE) was applied to yield a total passed charge of 50 mC (typical oxide weight was 50 μg). The same amount of Mn oxide was also deposited on a flat Ni substrate as a counterpart in this study. Electrochemical performance of the two electrodes was evaluated by cyclic voltammetry (CV) in 0.1 M Na₂SO₄ solution at 25 °C. The potential was scanned in a range of 0–0.9 V (versus SCE) with a rate of 5 mV s⁻¹. Moreover, cyclic stability of the electrodes was explored by repeating the test for 500 cycles; the cycling condition was the same as previously mentioned for the CV experiment. The capacitance decay versus the cycle number was recorded. The experimental details about the anodic deposition procedure and the electrochemical analysis method were reported in our previous papers [11,21].

3. Results and discussion

Fig. 1 shows a cyclic voltammogram for an ITO electrode in the plating solution with a potential scan rate of 10 mV s⁻¹. The equilibrium potentials for Cu and Ni in this solution are +0.04 and –0.50 V (versus SCE), respectively. On scanning the potential negative from the open-circuit potential (~0.20 V), the cathodic current onset at 0 V is followed by a reduction peak associated with the nucleation and growth of Cu. However, due to the low Cu(II) concentration in the solution, the deposition rate is under mass transfer control and does not significantly vary with potential. The onset of Ni(II) reduction is observed around –0.70 V. At more negative potentials, Ni and Cu are codeposited on the electrode and form an alloy [20,22]. On the reverse scan, the diffusion-limited deposition of Cu again occurs followed by two anodic peaks. The first peak located at 0.19 V is associated with the stripping of the pure Cu layer (deposited on the reverse scan). This presumption can be well supported by the inset of Fig. 1 which shows a CV curve with a negative scan limit of

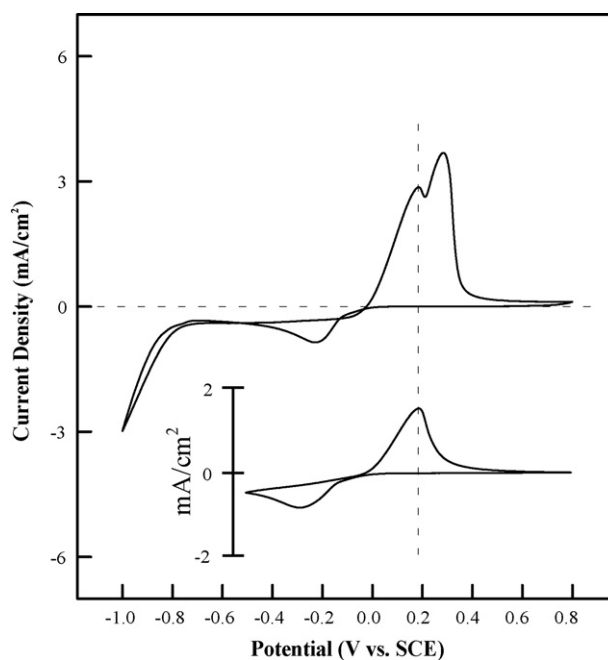


Fig. 1. Cyclic voltammogram for an ITO electrode in 1 M NiSO₄ + 0.01 M CuSO₄ + 0.5 M H₃BO₃ solution with a potential scan rate of 10 mV s⁻¹.

–0.50 V (no Ni can be deposited). The second peak at 0.23 V is mainly attributed to the selective etching of Cu in the alloy layer and also the dissolution of the underneath Cu layer deposited on the forward scan. It is found that the total charges integrated from the cathodic region were 50% higher than those of the anodic region. Since most Ni is passivated [20,23] (however, partial dissolution was observed in this study), it remains on the electrode. According to Fig. 1, electrodeposition of a Ni–Cu alloy film and selective dissolution of Cu from the alloy can be achieved in the same solution by simply switching the applied potential.

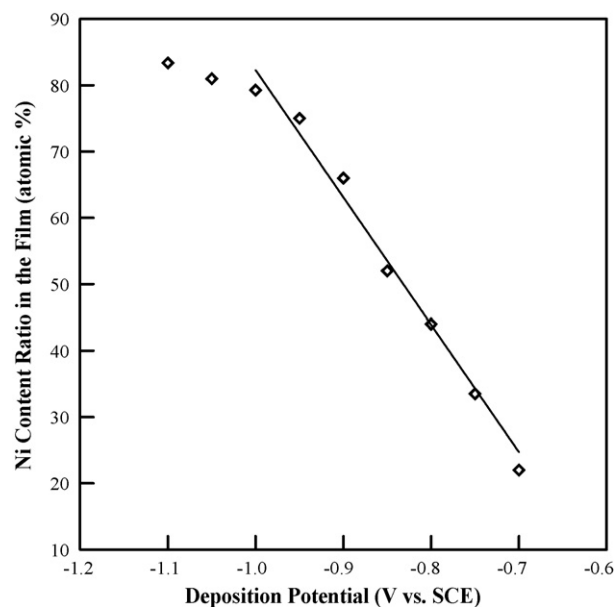


Fig. 2. Ni content ratios versus deposition potentials for the Ni–Cu alloy films.

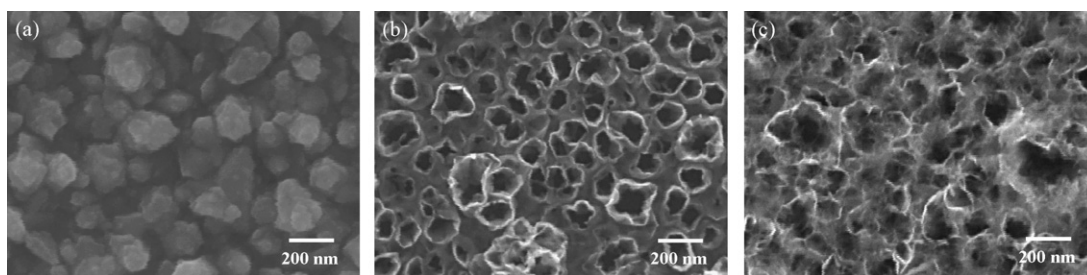


Fig. 3. SEM micrographs of the (a) as-deposited Ni–Cu alloy film, (b) nanoporous Ni film and (c) high-porosity Mn oxide electrode.

Fig. 2 shows an approximately linear relationship between the compositions of the prepared alloy films and their deposition potentials. At the potentials negative to -0.7 V, the Cu deposition is diffusion-limited and hence the rate is independent of potential, whereas the rate of Ni deposition increases with decreasing potential. As a result, the alloy film deposited at a more negative potential possesses a higher Ni content ratio. A slight deviation of the linear relationship below -1 V (revealed in Fig. 2) can be attributed to the hydrogen evolution. The wide range of Ni/Cu content ratios would enable a large variety of tailoring the porous structure of Ni while the Cu is selectively dissolved.

Fig. 3a shows a granular surface morphology of the as-deposited alloy film prepared at -0.85 V which has a Ni/Cu atomic ratio of approximately 50/50. Fig. 3b demonstrates a SEM photo of the alloy film after being etched at 0.5 V. Since the Cu within the alloy was selectively dissolved, the finely porous structure of Ni can be obtained. As seen in this figure, the pore sizes are in the range from 50 to 150 nm, and the pore density is about 10^{12} cm^{-2} . EDS analysis further confirmed that the residual Cu in the electrode was only about 5 at.%. A further study dealing with the pore formation mechanism is already underway and the results will be published elsewhere. Fig. 3c

exhibits a micrograph depicting the anodically deposited Mn oxide is loaded on this nanoporous Ni substrate. It is found that the fibrous Mn oxide with a nanosized diameter is sufficiently dispersed on the electrode surface, even inside the nanopores. Accordingly, a novel, efficient, and totally electrochemical process to prepare a high surface area Mn oxide electrode (with a nanoporous Ni substrate) is successfully proposed, as illustrated in the scheme shown in Fig. 4.

Fig. 5 shows the cyclic voltammograms of Mn oxides deposited on the prepared nanoporous Ni (curve a) and a flat Ni (curve b) substrates, measured in 0.1 M Na_2SO_4 electrolyte at 25 °C with a potential scan rate of 5 mV s^{-1} . The rectangular shapes and mirror-image characteristic of the CV curves reveal the ideal pseudocapacitive behavior of both the electrodes. However, it is found that the CV enclosed area, that correspond to charge storage capability, of the curve a is much larger than that of the curve b. The specific pseudocapacitance of the Mn oxide on a flat Ni substrates calculated [11,21] from Fig. 5 is 271 F g^{-1} , which is close to those typically reported in the literature [2,6–12]. In contrast, an exceptional oxide capacitance of 502 F g^{-1} (85% higher than the former one) can be achieved on the nanoporous Ni substrate. The high surface area of the conductive Ni substrate could expand the active sites for pseu-

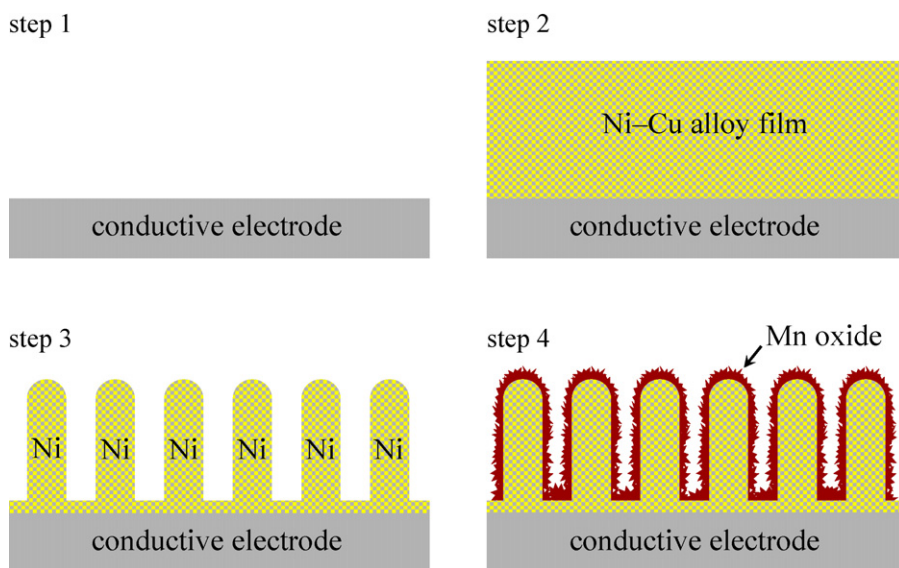


Fig. 4. Scheme of electrochemically preparing a high-porosity Mn oxide electrode. (Step 1) Any conductive material can be used as an electrode substrate. (Step 2) Ni and Cu are codeposited on the substrate and form an alloy film. (Step 3) Cu is selectively dissolved and Ni with a nanoporous structure is left. (Step 4) Fibrous Mn oxide is well-dispersed on the porous Ni by anodic deposition.

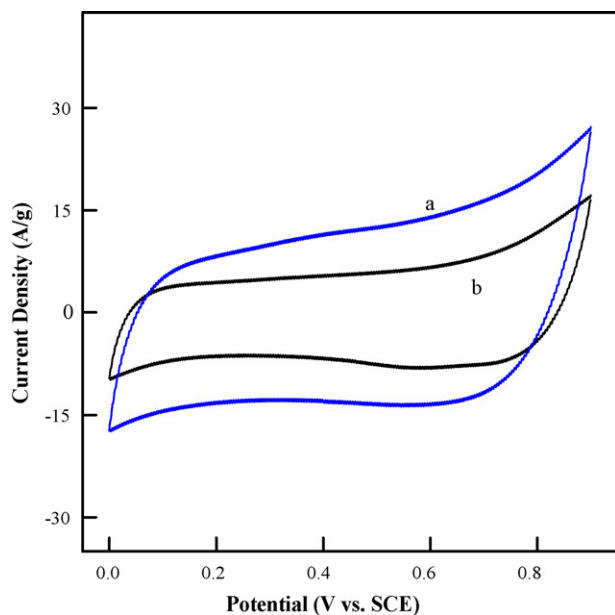


Fig. 5. Cyclic voltammograms of the Mn oxide electrodes with the nanoporous Ni substrate (curve a) and a flat Ni substrate (curve b). They were measured in 0.1 M Na_2SO_4 electrolyte at 25 °C with a potential scan rate of 5 mV s^{-1} .

docapacitive reaction and improve the utilization (or reactivity) of the Mn oxide. Moreover, the high-porosity structure of the Ni with the well-dispersed fibrous Mn oxide would enhance the accessibility of electrolyte and therefore promote the ionic transportation within the electrode. Accordingly, the excellent electrochemical performance can be obtained. The CV curve of the bare porous Ni electrode in the same electrolyte was also measured; no capacitive behavior with negligible current (as compared with the oxide electrode) was observed. This result indicated that the great improvement in capacitance of the porous oxide electrode was not associated with the double-layer capac-

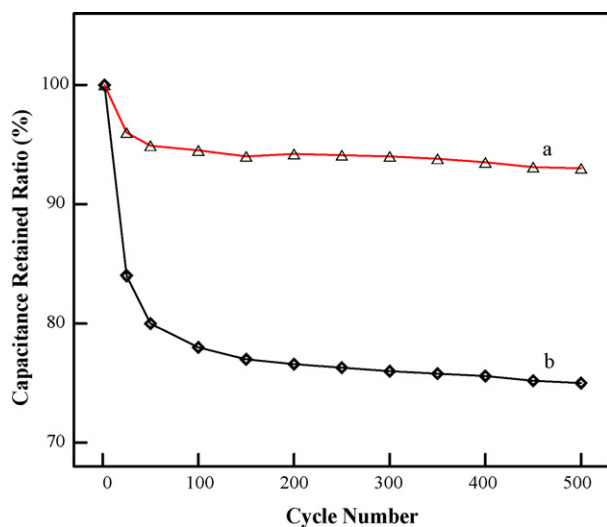


Fig. 6. Variations of specific capacitance versus CV cycle number for the Mn oxide electrodes with the nanoporous Ni substrate (curve a) and a flat Ni substrate (curve b). The tests were performed in 0.1 M Na_2SO_4 solution at 25 °C; the potential was scanned in a range of 0–0.9 V (vs. SCE) with a rate of 5 mV s^{-1} .

itance. Cyclic stability of the two electrodes is also evaluated by repeating the CV scan for 500 cycles, and the experimental data are shown in Fig. 6. The capacitance retained ratios of the Mn oxides deposited on the nanoporous Ni and a flat Ni substrates after the cycling tests were 93 and 75%, respectively. The superior cyclic stability of the former case was attributed to the better kinetic reversibility and electrochemical reaction homogeneity of the oxide electrode with its unique nanoporous structure. We believe that the nanoporous Ni substrate is applicable not only to Mn oxide, but also to other energy storage materials to improve their electrochemical performance.

4. Conclusions

A totally electrochemical process was first proposed in this study to fabricate a high-porosity (and high surface area) Mn oxide electrode with quite promising pseudocapacitive performance. Essentially, this preparation process is really simple and efficient, and it mainly includes three steps: (i) codeposition of a Ni–Cu alloy film on a conductive electrode. (ii) Selective dissolution of Cu from the alloy film and hence formation of a nanoporous Ni structure. (iii) Anodic deposition of fibrous Mn oxide onto the porous Ni substrate. The obtained oxide electrode can deliver an exceptional specific capacitance of 502 F g^{-1} , which is even better than those of the Mn oxides prepared with AAO and CNTs [13–19]. It was also noted that the cyclic stability of the high-porosity oxide electrode was greatly superior to that of a flat electrode.

Acknowledgement

The authors would like to thank the National Science Council of the Republic of China for financially supporting (Contract No. NSC 95-2221-E-006-192).

References

- [1] R. Kötz, M. Carlen, *Electrochim. Acta* 45 (2000) 2483–2498.
- [2] H.Y. Lee, J.B. Goodenough, *J. Solid State Chem.* 144 (1999) 220–223.
- [3] S.C. Pang, M.A. Anderson, T.W. Chapman, *J. Electrochem. Soc.* 147 (2000) 444–450.
- [4] M. Toupin, T. Brousse, D. Bélanger, *Chem. Mater.* 16 (2004) 3184–3190.
- [5] J.K. Chang, M.T. Lee, W.T. Tsai, *J. Power Sources* 166 (2007) 590–594.
- [6] H.Y. Lee, S.W. Kim, H.Y. Lee, *Electrochem. Solid State Lett.* 4 (2001) A19–A22.
- [7] M. Toupin, T. Brousse, D. Bélanger, *Chem. Mater.* 14 (2002) 3946–3952.
- [8] Y.U. Jeong, A. Manthiram, *J. Electrochem. Soc.* 149 (2002) A1419–A1422.
- [9] C.C. Hu, T.W. Tsou, *J. Power Sources* 115 (2003) 179–186.
- [10] H. Kim, B.N. Popov, *J. Electrochem. Soc.* 150 (2003) D56–D62.
- [11] J.K. Chang, W.T. Tsai, *J. Electrochem. Soc.* 150 (2003) A1333–A1338.
- [12] V. Subramanian, H. Zhu, R. Vajtai, P.M. Ajayan, B. Wei, *J. Phys. Chem. B* 109 (2005) 20207–20214.
- [13] W.C. West, N.V. Myung, J.F. Whitacre, B.V. Ratnakumar, *J. Power Sources* 126 (2004) 203–206.
- [14] X. Wang, X. Wang, W. Huang, P.J. Sebastian, S. Gamboa, *J. Power Sources* 140 (2005) 211–215.
- [15] C.L. Xu, S.J. Bao, L.B. Kong, H. Li, H.L. Li, *J. Solid State Chem.* 179 (2006) 1351–1355.

- [16] Y.T. Wu, C.C. Hu, *J. Electrochem. Soc.* 151 (2004) A2060–A2066.
- [17] Y.K. Zhou, B.L. He, F.B. Zhang, H.L. Li, *J. Solid State Electrochem.* 8 (2004) 482–487.
- [18] E. Raymundo-Pinero, V. Khomeiko, E. Frackowiak, F. Béguin, *J. Electrochem. Soc.* 152 (2005) A229–A235.
- [19] C.Y. Lee, H.M. Tsai, H.J. Chuang, S.Y. Li, P. Lin, T.Y. Tseng, *J. Electrochem. Soc.* 152 (2005) A716–A720.
- [20] L. Sun, C.L. Chien, P.C. Searson, *Chem. Mater.* 16 (2004) 3125–3129.
- [21] J.K. Chang, Y.L. Chen, W.T. Tsai, *J. Power Sources* 135 (2004) 344–353.
- [22] M. Zhou, N. Myung, X. Chen, K. Rajeshwar, *J. Electroanal. Chem.* 398 (1995) 5–12.
- [23] D.M. Tench, J.T. White, *J. Electrochem. Soc.* 137 (1990) 3061–3066.